

# $\bar{B}_s^0 \rightarrow K\pi, KK$ decays and effects of the next-to-leading order contributions

Jing-Jing Wang, Dong-Ting Lin, Wen Sun, Zhong-Jian Ji, Shan Cheng, and Zhen-Jun Xiao

*Department of Physics and Institute of Theoretical Physics,  
Nanjing Normal University, Nanjing, Jiangsu 210023, P.R.China*

(Dated: August 13, 2018)

By employing the perturbative QCD(pQCD) factorization approach, we calculate the branching ratios and CP violating asymmetries of the four  $\bar{B}_s^0 \rightarrow K\pi$  and  $KK$  decays, with the inclusion of all known next-to-leading order (NLO) contributions. We find numerically that (a) the NLO contribution can interfere with the LO part constructively or destructively for different decay modes; (b) the NLO contribution leads to a 22% decrease for  $Br(\bar{B}_s^0 \rightarrow K^+\pi^-)$ , but  $\sim 50\%$  enhancements to other three considered  $\bar{B}_s$  decays, and therefore play an important role in interpreting the measured values of the branching ratios; and (c) for both  $\bar{B}_s^0 \rightarrow K^+\pi^-$  and  $\bar{B}_s^0 \rightarrow K^+K^-$  decays, the NLO pQCD predictions for the direct and mixing induced CP-violating asymmetries agree very well with the measured values in both the sign and the magnitude.

## I. INTRODUCTION

The  $B$  and  $B_s$  decays are very interesting phenomenologically for the precision test of the standard model (SM) and for the searches for the signal of the new physics beyond the SM. But the  $B_s$  decays are considerably less studied than the well-known  $B_{u,d}$  decays due to the rapid oscillations of  $B_s$  mesons and the shortage of  $B_s$  events collected. Since the start of the LHC running, a lot of  $B_s^0$  events have been collected by LHCb collaboration, and some  $B_s^0 \rightarrow PP$  decays are already observed [1, 2]: such as the first observation of the direct CP violation in  $B_s$  decays [1]:

$$A_{CP}(B_s^0 \rightarrow K^-\pi^+) = (0.27 \pm 0.04(stat) \pm 0.01(syst)), \quad (1)$$

and the first measurement of the time-dependent CP violation in  $B_s^0 \rightarrow K^+K^-$  [2]:

$$\begin{aligned} C_{KK} &= 0.14 \pm 0.11(stat) \pm 0.03(syst), \\ S_{KK} &= 0.30 \pm 0.12(stat) \pm 0.04(syst). \end{aligned} \quad (2)$$

During the past decade, in fact, many charmless two-body hadronic  $B_s^0 \rightarrow M_2M_3$  decays have been studied by employing the pQCD factorization approach at the LO level [3–5] or the partial NLO level [6]. In this paper we calculate the branching ratios and CP violating asymmetries of the  $B_s^0 \rightarrow K\pi$  and  $KK$  decays by employing the pQCD factorization approach, with the inclusion of all known NLO contributions. These decay modes have also been studied, for example, by using the pQCD approach at the LO level in Ref. [5], the generalized factorization in Ref. [7] or by using the QCD factorization approach in Ref. [8–10].

In the pQCD factorization approach, almost all NLO contributions to  $B_{u,d} \rightarrow M_2M_3$  decays have been calculated up to now. And it is straightforward to extend these calculations to the cases for the similar  $B_s \rightarrow M_2M_3$  decays. The NLO pQCD predictions for those considered decay modes proved that the NLO contributions can play an important role in understanding the very large  $Br(B \rightarrow K\eta')$  [11, 12] or the so-called “ $K\pi$ -puzzle” [13]. We here focus on the studies

for the possible effects of the NLO contributions from various sources: such as the QCD vertex corrections (VC), the quark-loops (QL) and the chromo-magnetic penguins (CMP) [8, 14]. The newly known NLO twist-2 contribution [15] and NLO twist-3 contribution to the relevant form factors [16] will also be taken into account here. By this way, one can improve the reliability of the pQCD factorization approach effectively.

This paper is organized as follows. In Sec. II, we give a brief review about the pQCD factorization approach and present the LO decay amplitudes for the studied decay modes. In Sec. III, the NLO contributions from different sources are evaluated analytically. We calculate and show the pQCD predictions for the branching ratios and CP violating asymmetries of  $B_s^0 \rightarrow K\pi$  and  $KK$  decays in Sec. IV. The summary and some discussions are included in the final section.

## II. THEORETICAL FRAMEWORK AND LO DECAY AMPLITUDES

### A. Outlines of the pQCD approach

We consider the  $B$  meson at rest for simplicity. Using the light-cone coordinates, we define the  $B_s^0$  meson with momentum  $P_1$ , the emitted meson  $M_2$  with momentum  $P_2$  moving along the direction of  $n = (1, 0, \mathbf{0}_T)$  and the recoiled meson  $M_3$  with momentum  $P_3$  in the direction of  $v = (0, 1, \mathbf{0}_T)$ . Here we also use  $x_i$  to denote the momentum fraction of anti-quark in each meson:

$$P_1 = \frac{m_{B_s}}{\sqrt{2}}(1, 1, \mathbf{0}_T), \quad P_2 = \frac{m_{B_s}}{\sqrt{2}}(1 - r_3^2, r_2^2, \mathbf{0}_T), \quad P_3 = \frac{m_{B_s}}{\sqrt{2}}(r_3^2, 1 - r_2^2, \mathbf{0}_T), \quad (3)$$

$$k_1 = \frac{m_{B_s}}{\sqrt{2}}(x_1, 0, \mathbf{k}_{1T}), \quad k_2 = \frac{m_{B_s}}{\sqrt{2}}(x_2(1 - r_3^2), x_2 r_2^2, \mathbf{k}_{2T}),$$

$$k_3 = \frac{m_{B_s}}{\sqrt{2}}(x_3 r_3^2, x_3(1 - r_2^2), \mathbf{k}_{3T}), \quad (4)$$

where  $r_i = m_i/m_{B_s}$  with  $m_i = m_\pi$  or  $m_K$  here. When the light pion and kaon are the final state mesons,  $r_i^2 < 0.01$  and can be neglected safely. The integration over the small components  $k_1^-$ ,  $k_2^-$ , and  $k_3^-$  will lead conceptually to the decay amplitudes,

$$\mathcal{A}(B_s \rightarrow M_2 M_3) \sim \int dx_1 dx_2 dx_3 b_1 db_1 b_2 db_2 b_3 db_3$$

$$\cdot \text{Tr} [C(t)\Phi_{B_s}(x_1, b_1)\Phi_{M_2}(x_2, b_2)\Phi_{M_3}(x_3, b_3)H(x_i, b_i, t)S_t(x_i) e^{-S(t)}], \quad (5)$$

where  $b_i$  is the conjugate space coordinate of  $k_{iT}$ . In the above equation,  $C(t)$  is the Wilson coefficient evaluated at scale  $t$ . The functions  $\Phi_{B_s}$ ,  $\Phi_{M_2}$  and  $\Phi_{M_3}$  are the wave functions of the initial  $B_s$  meson and the final-state meson  $M_2$  and  $M_3$  respectively. The hard kernel  $H(k_1, k_2, k_3, t)$  describes the four-quark operator and the spectator quark connected by a hard gluon whose  $q^2$  is in the order of  $\bar{\Lambda}m_{B_s}$ . The jet function  $S_t(x_i)$  in Eq.(5) is one of the two kinds of Sudakov form factors relevant for the  $B_s$  decays considered, which come from the threshold resummation over the large double logarithms ( $\ln^2 x_i$ ) in the end-point region. The function  $e^{-S(t)}$  is the second kind of the Sudakov form factors. The Sudakov form factors suppress effectively the soft dynamics at the end-point region [17].

For the studied  $\bar{B}_s^0 \rightarrow K\pi, KK$  decays, the corresponding weak effective Hamiltonian can be written as [18]

$$\mathcal{H}_{eff} = \frac{G_F}{\sqrt{2}} \left\{ V_{ub}V_{uq}^* \left[ C_1(\mu)O_1^u(\mu) + C_2(\mu)O_2^u(\mu) \right] - V_{tb}V_{tq}^* \left[ \sum_{i=3}^{10} C_i(\mu)O_i(\mu) \right] \right\} + \text{h.c.}, \quad (6)$$

where  $q = d, s$ ,  $G_F = 1.16639 \times 10^{-5} \text{GeV}^{-2}$  is the Fermi constant, and  $V_{ij}$  is the Cabbibo-Kobayashi-Maskawa (CKM) matrix element,  $C_i(\mu)$  are the Wilson coefficients evaluated at the renormalization scale  $\mu$  and  $O_i(\mu)$  are the four-fermion operators.

As usual, we treat the  $B$  meson as a very good heavy-light system, and adopt the distribution amplitude  $\phi_{B_s}$  as in Ref. [5]

$$\phi_{B_s}(x, b) = N_{B_s} x^2 (1-x)^2 \exp \left[ -\frac{M_{B_s}^2 x^2}{2\omega_b^2} - \frac{1}{2}(\omega_b b)^2 \right], \quad (7)$$

where the shape parameter  $\omega_b$  is a free parameter and we take  $\omega_b = 0.5 \pm 0.05 \text{ GeV}$  for  $B_s$  meson based on studies of lattice QCD and light-cone sum rule[17], and finally the normalization factor  $N_{B_s}$  depends on the values of  $\omega_b$  and the decay constant  $f_{B_s}$  and defined through the normalization relation  $\int_0^1 dx \phi_{B_s}(x, 0) = f_{B_s}/(2\sqrt{6})$ .

For the light pseudo-scalar mesons  $\pi$  and  $K$ , their wave functions are the same in form and can be defined as [19]

$$\Phi(P, x, \zeta) \equiv \frac{1}{\sqrt{2N_C}} \gamma_5 \left[ \not{P} \phi^A(x) + m_0 \phi^P(x) + \zeta m_0 (\not{p} - 1) \phi_P^T(x) \right], \quad (8)$$

where  $P$  and  $x$  are the momentum of the light meson and the momentum fraction of the quark (or anti-quark) inside the meson, respectively. When the momentum fraction of the quark (anti-quark) is set to be  $x$ , the parameter  $\zeta$  should be chosen as  $+1$  ( $-1$ ). The distribution amplitudes (DA's) of the light meson  $M = (\pi, K)$  are adopted from Ref. [19, 20]:

$$\phi_M^A(x) = \frac{3f_M}{\sqrt{6}} x(1-x) \left[ 1 + a_1^M C_1^{3/2}(t) + a_2^M C_2^{3/2}(t) \right], \quad (9)$$

$$\phi_M^P(x) = \frac{f_M}{2\sqrt{6}} \left[ 1 + \left( 30\eta_3 - \frac{5}{2}\rho_M^2 \right) C_2^{1/2}(t) \right], \quad (10)$$

$$\phi_M^T(x) = \frac{f_M(1-2x)}{2\sqrt{6}} \left[ 1 + 6 \left( 5\eta_3 - \frac{1}{2}\eta_3\omega_3 - \frac{7}{20}\rho_M^2 - \frac{3}{5}\rho_M^2 a_2^M \right) (1 - 10x + 10x^2) \right], \quad (11)$$

with the mass ratio  $\rho_M = (m_\pi/m_0^\pi, m_K/m_0^K)$  for  $M = (\pi, K)$  respectively [11, 14]. The Gegenbauer moments  $a_i^M$  and other input parameters are the same as in Ref. [5]:

$$\begin{aligned} a_1^\pi &= 0, & a_2^\pi &= 0.44_{-0.20}^{+0.10}, & a_1^K &= 0.17 \pm 0.05, & a_2^K &= 0.20 \pm 0.06, \\ \eta_3 &= 0.015, & \omega_3 &= -3.0. \end{aligned} \quad (12)$$

The Gegenbauer polynomials  $C_n^\nu(t)$  in Eqs. (9-11) can be found easily in Refs. [5, 12]. For more details about recent progress on the wave functions of heavy and light mesons, one can see Ref. [21] and references therein.

## B. Decay amplitudes at leading order

The four  $\bar{B}_s^0 \rightarrow (K^+\pi^-, K^0\pi^0, K^+K^-, \bar{K}^0 K^0)$  decays have been studied previously in Ref. [5] by employing the pQCD factorization approach at leading order. The decay amplitudes as presented in Ref.[5] are confirmed by our recalculation. In this paper, we focus on the calculations of the NLO contributions to these decays. At the leading order, the relevant Feynman diagrams which may contribute to the  $B_s^0 \rightarrow K\pi, KK$  decays are illustrated in Fig. 1. For the sake of

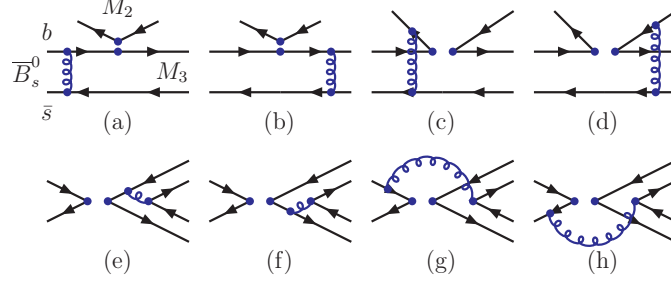


FIG. 1. Typical Feynman diagrams which may contribute at leading order to  $\bar{B}_s^0 \rightarrow K\pi, KK$  decays.

completeness, however, we firstly show the relevant LO decay amplitudes in this section based on our own analytical calculations.

$$\begin{aligned} \mathcal{A}(\bar{B}_s^0 \rightarrow K^+\pi^-) &= V_{ub}V_{ud}^* \cdot [f_\pi F_{eK} a_1 + M_{eK} C_1] - V_{tb}V_{td}^* \cdot \left\{ f_\pi F_{eK} (a_4 + a_{10}) \right. \\ &\quad \left. + f_\pi F_{eK}^{P_2} (a_6 + a_8) + M_{eK} (C_3 + C_9) + f_{B_s} F_{aK} \left( a_4 - \frac{1}{2} a_{10} \right) \right. \\ &\quad \left. + f_{B_s} F_{aK}^{P_2} \left( a_6 - \frac{1}{2} a_8 \right) + M_{aK} \left( C_3 - \frac{1}{2} C_9 \right) + M_{aK}^{P_1} \left( C_5 - \frac{1}{2} C_7 \right) \right\}, \quad (13) \end{aligned}$$

$$\begin{aligned} \sqrt{2}\mathcal{A}(\bar{B}_s^0 \rightarrow K^0\pi^0) &= V_{ub}V_{ud}^* \cdot [f_\pi F_{eK} a_2 + M_{eK} C_2] - V_{tb}V_{td}^* \cdot \left\{ -f_{B_s} F_{aK} \left( a_4 - \frac{1}{2} a_{10} \right) \right. \\ &\quad \left. - (f_\pi F_{eK}^{P_2} + f_{B_s} F_{aK}^{P_2}) \left( a_6 - \frac{1}{2} a_8 \right) + M_{eK} \left( -C_3 + \frac{3}{2} C_8 + \frac{1}{2} C_9 + \frac{3}{2} C_{10} \right) \right. \\ &\quad \left. + f_\pi F_{eK} \left( -a_4 - \frac{3}{2} a_7 + \frac{3}{2} a_9 + \frac{1}{2} a_{10} \right) - M_{aK} \left( C_3 - \frac{1}{2} C_9 \right) - M_{aK}^{P_1} \left( C_5 - \frac{1}{2} C_7 \right) \right\}, \quad (14) \end{aligned}$$

$$\begin{aligned} \mathcal{A}(\bar{B}_s^0 \rightarrow K^+K^-) &= V_{ub}V_{us}^* \cdot [f_k F_{eK} a_1 + M_{eK} C_1 + M_{aK} C_2] - V_{tb}V_{ts}^* \cdot \left\{ f_k F_{eK} (a_4 + a_{10}) \right. \\ &\quad \left. + f_k F_{eK}^{P_2} (a_6 + a_8) + M_{eK} (C_3 + C_9) + M_{eK}^{P_1} (C_5 + C_7) + f_{B_s} F_{aK}^{P_2} \left( a_6 - \frac{1}{2} a_8 \right) \right. \\ &\quad \left. + M_{aK} \left( C_3 + C_4 - \frac{1}{2} C_9 - \frac{1}{2} C_{10} \right) + M_{aK}^{P_1} \left( C_5 - \frac{1}{2} C_7 \right) \right. \\ &\quad \left. M_{aK}^{P_2} \left( C_6 - \frac{1}{2} C_8 \right) + [M_{aK} (C_4 + C_{10}) + M_{aK}^{P_2} (C_6 + C_8)]_{K^+ \leftrightarrow K^-} \right\}, \quad (15) \end{aligned}$$

$$\begin{aligned} \mathcal{A}(\bar{B}_s^0 \rightarrow \bar{K}^0 K^0) &= -V_{tb}V_{ts}^* \cdot \left\{ f_k F_{eK} \left( a_4 - \frac{1}{2} a_{10} \right) + (f_k F_{eK}^{P_2} + f_{B_s} F_{aK}^{P_2}) \left( a_6 - \frac{1}{2} a_8 \right) \right. \\ &\quad \left. + M_{eK} \left( C_3 - \frac{1}{2} C_9 \right) + (M_{eK}^{P_1} + M_{aK}^{P_1}) \left( C_5 - \frac{1}{2} C_7 \right) + M_{aK} \left( C_3 + C_4 - \frac{1}{2} C_9 - \frac{1}{2} C_{10} \right) \right. \\ &\quad \left. + M_{aK} \left( C_4 - \frac{1}{2} C_{10} \right)_{K^0 \leftrightarrow \bar{K}^0} + \left[ M_{aK}^{P_2} \left( C_6 - \frac{1}{2} C_8 \right) + [K^0 \leftrightarrow \bar{K}^0] \right] \right\}, \quad (16) \end{aligned}$$

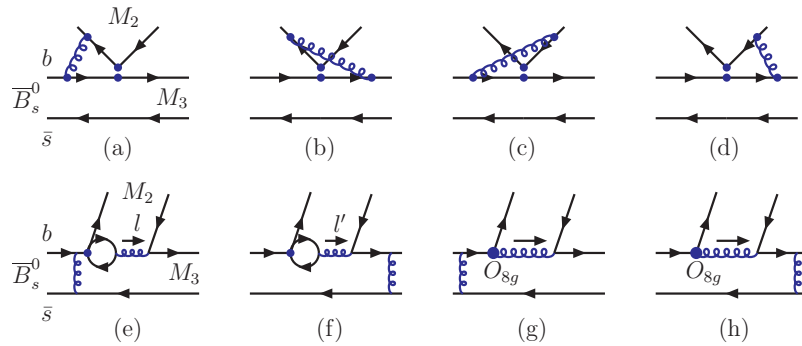


FIG. 2. Feynman diagrams for NLO contributions: the vertex corrections (a-d); the quark-loop (e-f) and the chromo-magnetic penguin contributions (g-h).

where  $a_i$  is the combination of the Wilson coefficients  $C_i$  the same as in Ref. [5]. The nine individual decay amplitudes, such as  $F_{eK}$  and  $F_{eK}^{P2}$  appeared in Eqs. (13-16), are obtained by evaluating the corresponding Feynman diagrams in Fig. 1 analytically. One can find the expressions for all these decay amplitudes easily in Ref. [5].

### III. NEXT-TO-LEADING ORDER CONTRIBUTIONS

#### A. NLO contributions from different sources

For the considered decay modes, one should, firstly, use the NLO Wilson coefficients  $C_i(M_W)$ , the NLO RG evolution matrix  $U(t, m, \alpha)$  [18] and the  $\alpha_s(t)$  at two-loop level in numerical calculations. Secondly, one should take all the Feynman diagrams which lead to the decay amplitudes proportional to  $\alpha_s^2(t)$  in the analytical evaluations. Such Feynman diagrams can be grouped into following classes:

1. The vertex corrections, as illustrated in Figs. 2a-2d, the same set as in the QCDF approach.
2. The NLO contributions from quark-loops [14] and the chromo-magnetic penguin operator  $O_{8g}$  [22], as illustrated in Figs. 2e-2h.
3. The NLO contributions to the form factors of  $B \rightarrow K$  transitions [15, 16], coming from the Feynman diagrams in Fig. 3.
4. The NLO corrections to the LO hard spectator diagrams and annihilation diagrams, as illustrated in Fig. 5 of Ref.[12].

At present, only the calculations for the NLO corrections to the LO hard spectator and annihilation diagrams have not been completed yet. But from the comparative studies of the LO and NLO contributions from different sources in Ref. [12, 13], we believe that those still unknown NLO contributions in the framework of the pQCD factorization approach, as the high order corrections to small LO contributions, are most possibly very small in size and could be neglected safely.

The vertex corrections to the factorizable emission diagrams, as illustrated by Figs. 2a-2d, have been calculated years ago in the QCD factorization approach [8, 23]. For  $B_s^0 \rightarrow K\pi, KK$  decays, the vertex corrections can be calculated without considering the transverse momentum effects of the quark at the end-point [14], one can use the vertex corrections as given in Ref. [8] directly. The vertex corrections can then be absorbed into the re-definition of the Wilson coefficients  $a_i(\mu)$

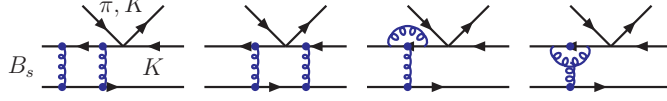


FIG. 3. The four typical Feynman diagrams, which contribute to the form factors of  $B \rightarrow M_3$  transitions at NLO level.

by adding a vertex-function  $V_i(M)$  to them. The expressions of the vertex functions  $V_i(M)$  can be found easily in Refs. [8, 14].

The contribution from the so-called ‘‘quark-loops’’ is a kind of penguin correction with the four quark operators insertion, as illustrated by Fig. 2e and 2f. For the  $b \rightarrow s$  transition, the effective Hamiltonian  $H_{eff}^{ql}$  which describes the contributions from the quark loops can be written as [14]

$$H_{eff}^{(QL)} = - \sum_{q=u,c,t} \sum_{q'} \frac{G_F}{\sqrt{2}} V_{qb} V_{qs}^* \frac{\alpha_s(\mu)}{2\pi} C^{(q)}(\mu, l^2) (\bar{s} \gamma_\rho (1 - \gamma_5) T^a b) (\bar{q}' \gamma^\rho T^a q'), \quad (17)$$

where  $l^2$  is the invariant mass of the gluon, as illustrated by Fig.2e. The expressions of the functions  $C^{(q)}(\mu, l^2)$  for the loop of the  $q$  ( $q = u, d, s, c, t$ ) quark can be found for example in Ref. [14].

The magnetic penguin is another kind penguin correction induced by the insertion of the operator  $O_{8g}$ , as illustrated by Fig.2g and 2h. The corresponding weak effective Hamiltonian contains the  $b \rightarrow sg$  transition can be written as

$$H_{eff}^{MP} = - \frac{G_F}{\sqrt{2}} V_{tb} V_{ts}^* C_{8g}^{eff} O_{8g}, \quad (18)$$

where  $O_{8g}$  is the chromo-magnetic penguin operator [18, 22] and  $C_{8g}^{eff}$  is the corresponding effective Wilson coefficient:  $C_{8g}^{eff} = C_{8g} + C_5$  [14].

In Refs. [15, 16], the authors calculated the NLO twist-2 and twist-3 contributions to the form factors  $f^{+,0}(q^2)$  of the  $B \rightarrow \pi$  transition. The NLO pQCD prediction for the form factor  $f^+(q^2)$ , for example, is of the form [16]

$$\begin{aligned} f^+(q^2)|_{\text{NLO}} = & 8\pi m_B^2 C_F \int dx_1 dx_2 \int b_1 db_1 b_2 db_2 \phi_B(x_1, b_1) \\ & \times \left\{ r_\pi [\phi_\pi^P(x_2) - \phi_\pi^T(x_2)] \cdot \alpha_s(t_1) \cdot e^{-S_{B\pi}(t_1)} \cdot S_t(x_2) \cdot h(x_1, x_2, b_1, b_2) \right. \\ & + \left[ (1 + x_2 \eta) \left( 1 + F_{T2}^{(1)}(x_i, \mu, \mu_f, q^2) \right) \phi_\pi^A(x_2) + 2r_\pi \left( \frac{1}{\eta} - x_2 \right) \phi_\pi^T(x_2) \right. \\ & \left. \left. - 2x_2 r_\pi \phi_\pi^P(x_2) \right] \cdot \alpha_s(t_1) \cdot e^{-S_{B\pi}(t_1)} \cdot S_t(x_2) \cdot h(x_1, x_2, b_1, b_2) \right. \\ & + 2r_\pi \phi_\pi^P(x_2) \left( 1 + F_{T3}^{(1)}(x_i, \mu, \mu_f, q^2) \right) \\ & \left. \left. \cdot \alpha_s(t_2) \cdot e^{-S_{B\pi}(t_2)} \cdot S_t(x_2) \cdot h(x_2, x_1, b_2, b_1) \right\}, \quad (19) \end{aligned}$$

where  $\eta = 1 - q^2/m_B^2$  with  $q^2 = (P_B - P_\pi)^2$ ,  $\mu$  ( $\mu_f$ ) is the renormalization (factorization) scale, the hard scale  $t_{1,2}$  are chosen as the largest scale of the propagators in the hard  $b$ -quark decay diagrams [15, 16], the function  $S_t(x_2)$  is the threshold resummation factor adopted from Ref. [24],

the expressions of the hard function  $h(x_i, b_j)$  can be found in Ref. [15, 16], and finally the factor  $F_{T_2}^{(1)}(x_i, \mu, \mu_f, q^2)$  and  $F_{T_3}^{(1)}(x_i, \mu, \mu_f, q^2)$  describe the NLO twist-2 and twist-3 contribution to  $f^{+,0}(q^2)$  of the  $B \rightarrow \pi$  transition respectively [15, 16]:

$$\begin{aligned}
F_{T_2}^{(1)}(x_i, \mu, \mu_f, q^2) = & \frac{\alpha_s(\mu_f)C_F}{4\pi} \left[ \frac{21}{4} \ln \frac{\mu^2}{m_B^2} - \left( \frac{13}{2} + \ln r_1 \right) \ln \frac{\mu_f^2}{m_B^2} + \frac{7}{16} \ln^2(x_1 x_2) + \frac{1}{8} \ln^2 x_1 \right. \\
& + \frac{1}{4} \ln x_1 \ln x_2 + \left( -\frac{1}{4} + 2 \ln r_1 + \frac{7}{8} \ln \eta \right) \ln x_1 + \left( -\frac{3}{2} + \frac{7}{8} \ln \eta \right) \ln x_2 \\
& \left. + \frac{15}{4} \ln \eta - \frac{7}{16} \ln^2 \eta + \frac{3}{2} \ln^2 r_1 - \ln r_1 + \frac{101\pi^2}{48} + \frac{219}{16} \right], \tag{20}
\end{aligned}$$

$$\begin{aligned}
F_{T_3}^{(1)}(x_i, \mu, \mu_f, q^2) = & \frac{\alpha_s(\mu_f)C_F}{4\pi} \left[ \frac{21}{4} \ln \frac{\mu^2}{m_B^2} - \frac{1}{2}(6 + \ln r_1) \ln \frac{\mu_f^2}{m_B^2} + \frac{7}{16} \ln^2 x_1 - \frac{3}{8} \ln^2 x_2 \right. \\
& + \frac{9}{8} \ln x_1 \ln x_2 + \left( -\frac{29}{8} + \ln r_1 + \frac{15}{8} \ln \eta \right) \ln x_1 + \left( -\frac{25}{16} + \ln r_2 + \frac{9}{8} \ln \eta \right) \ln x_2 \\
& \left. + \frac{1}{2} \ln r_1 - \frac{1}{4} \ln^2 r_1 + \ln r_2 - \frac{9}{8} \ln \eta - \frac{1}{8} \ln^2 \eta + \frac{37\pi^2}{32} + \frac{91}{32} \right], \tag{21}
\end{aligned}$$

where  $r_i = m_B^2/\xi_i^2$  with the choice of  $\xi_1 = 25m_B$ [15]. According to the analytical and numerical evaluations in Ref. [16], we get to know that the NLO twist-2 and NLO twist-3 contribution to the form factor of  $B \rightarrow \pi$  transition are similar in size but have an opposite sign, which leads to a strong cancelation between them and consequently results in a small total NLO contribution,  $\sim 7\%$  variation to the full LO pQCD prediction for the case of  $f^+(q^2)$  in the range of  $0 \leq q^2 \leq 12 \text{ GeV}^2$ , as illustrated explicitly in Fig. 8 of Ref. [16].

In this paper we adopt the above NLO factors  $F_{T_2}^{(1)}(x_i, \mu, \mu_f, q^2)$  and  $F_{T_3}^{(1)}(x_i, \mu, \mu_f, q^2)$  directly, and then extend the expressions to the case for  $B \rightarrow K$  transition under the assumption of  $SU(3)$  flavor symmetry, by making the proper replacements, such as  $r_\pi = m_\pi/m_B \rightarrow r_k = m_k/m_{B_s}$ ,  $m_B \rightarrow m_{B_s}$  and  $\phi_\pi^{A,P,T} \rightarrow \phi_K^{A,P,T}$ , for the expressions as given in Eqs. (20,21).

## B. NLO decay amplitudes

For the sake of comparison and convenience we denote all currently known NLO contributions except for those NLO twist-2 and twist-3 contributions to the form factors by the label ‘‘Set-A’’, as described in previous subsection. For the four considered  $B_s^0 \rightarrow K\pi, KK$  decays, the Set-A NLO contributions will be included in a simple way:

$$\mathcal{A}_{K\pi} \rightarrow \mathcal{A}_{K\pi} + \sum_{q=u,c,t} V_{qb}V_{qd}^* \mathcal{M}_{K^+\pi^-}^{(QL)} + V_{tb}V_{td}^* \mathcal{M}_{K^+\pi^-}^{(MP)}, \tag{22}$$

$$\mathcal{A}_{KK} \rightarrow \mathcal{A}_{KK} + \sum_{q=u,c,t} V_{qb}V_{qs}^* \mathcal{M}_{K^+K^-}^{(QL)} + V_{tb}V_{ts}^* \mathcal{M}_{K^+K^-}^{(MP)}, \tag{23}$$

where the quark-loop and magnetic penguin amplitudes  $\mathcal{M}_{XY}^{(QL)}$  and  $\mathcal{M}_{XY}^{(MP)}$  are of the form

$$\begin{aligned} \mathcal{M}_{K^+\pi^-}^{(QL)} = & -8m_{B_s}^4 \frac{C_F^2}{\sqrt{6}} \int_0^1 dx_1 dx_2 dx_3 \int_0^\infty b_1 db_1 b_3 db_3 \phi_{B_s}(x_1) \\ & \times \left\{ \left[ (1+x_3) \phi_\pi^A(x_2) \phi_K^A(x_3) + r_K (1-2x_3) \phi_\pi^A(x_2) (\phi_K^P(x_3) + \phi_K^T(x_3)) \right. \right. \\ & \left. \left. + 2r_\pi \phi_\pi^P(x_2) \phi_K^A(x_3) \right] \cdot \alpha_s^2(t_a) \cdot h_e(x_1, x_3, b_1, b_3) \cdot \exp[-S_{ab}(t_a)] \cdot C^{(q)}(t_a, l^2) \right. \\ & \left. \left. + 2r_K \phi_\pi^A(x_2) \phi_K^P(x_3) \cdot \alpha_s^2(t_b) \cdot h_e(x_3, x_1, b_3, b_1) \exp[-S_{ab}(t_b)] \cdot C^{(q)}(t_b, l'^2) \right\}, \quad (24) \end{aligned}$$

$$\begin{aligned} \mathcal{M}_{K^+\pi^-}^{(MP)} = & -16m_{B_s}^6 \frac{C_F^2}{\sqrt{6}} \int_0^1 dx_1 dx_2 dx_3 \int_0^\infty b_1 db_1 b_2 db_2 b_3 db_3 \phi_{B_s}(x_1) \\ & \cdot \left\{ \left[ (1-x_3) \phi_\pi^A(x_2) [2\phi_K^A(x_3) + r_K(3+x_3)\phi_K^P(x_3) + r_K(1-x_3)\phi_K^T(x_3)] \right. \right. \\ & \left. \left. - r_\pi x_2 (1+x_3) (3\phi_\pi^P(x_2) - \phi_\pi^T(x_2)) \phi_K^A(x_3) \right] \right. \\ & \left. \cdot \alpha_s^2(t_a) \cdot h_g(x_i, b_i) \cdot \exp[-S_{cd}(t_a)] \cdot C_{8g}^{eff}(t_a) \right. \\ & \left. \left. + 4r_K \phi_\pi^A(x_2) \phi_K^P(x_3) \cdot \alpha_s^2(t_b) h'_g(x_i, b_i) \cdot \exp[-S_{cd}(t_b)] \cdot C_{8g}^{eff}(t_b) \right\}, \quad (25) \end{aligned}$$

$$\sqrt{2}\mathcal{M}_{K^0\pi^0}^{(QL)} = \mathcal{M}_{\pi^-K^+}^{(QL)}, \quad \sqrt{2}\mathcal{M}_{K^0\pi^0}^{(MP)} = \mathcal{M}_{\pi^-K^+}^{(MP)}, \quad (26)$$

$$\begin{aligned} \mathcal{M}_{K^+K^-}^{(QL)} = & -8m_{B_s}^4 \frac{C_F^2}{\sqrt{6}} \int_0^1 dx_1 dx_2 dx_3 \int_0^\infty b_1 db_1 b_3 db_3 \phi_{B_s}(x_1) \\ & \times \left\{ \left[ (1+x_3) \phi_K^A(x_2) \phi_K^A(x_3) + r_K (1-2x_3) \phi_K^A(x_2) (\phi_K^P(x_3) + \phi_K^T(x_3)) \right. \right. \\ & \left. \left. + 2r_K \phi_K^P(x_2) \phi_K^A(x_3) \right] \cdot \alpha_s^2(t_a) \cdot h_e(x_1, x_3, b_1, b_3) \cdot \exp[-S_{ab}(t_a)] \cdot C^{(q)}(t_a, l^2) \right. \\ & \left. \left. + 2r_K \phi_K^A(x_2) \phi_K^P(x_3) \cdot \alpha_s^2(t_b) \cdot h_e(x_3, x_1, b_3, b_1) \cdot \exp[-S_{ab}(t_b)] \cdot C^{(q)}(t_b, l'^2) \right\}, \quad (27) \end{aligned}$$

$$\begin{aligned} \mathcal{M}_{K^+K^-}^{(MP)} = & -16m_{B_s}^6 \frac{C_F^2}{\sqrt{6}} \int_0^1 dx_1 dx_2 dx_3 \int_0^\infty b_1 db_1 b_2 db_2 b_3 db_3 \phi_{B_s}(x_1) \\ & \cdot \left\{ \left[ (1-x_3) [2\phi_K^A(x_3) + r_K(3\phi_K^P(x_3) + \phi_K^T(x_3)) + r_K x_3 (\phi_K^P(x_3) - \phi_K^T(x_3))] \phi_K^A(x_2) \right. \right. \\ & \left. \left. - r_K x_2 (1+x_3) (3\phi_K^P(x_2) - \phi_K^T(x_2)) \phi_K^A(x_3) \right] \right. \\ & \left. \cdot \alpha_s^2(t_a) \cdot h_g(x_i, b_i) \cdot \exp[-S_{cd}(t_a)] \cdot C_{8g}^{eff}(t_a) \right. \\ & \left. \left. + 4r_K \phi_K^A(x_2) \phi_K^P(x_3) \cdot \alpha_s^2(t_b) \cdot h'_g(x_i, b_i) \cdot \exp[-S_{cd}(t_b)] \cdot C_{8g}^{eff}(t_b) \right\}, \quad (28) \end{aligned}$$

$$\mathcal{M}_{\bar{K}^0 K^0}^{(QL)} = \mathcal{M}_{K^+K^-}^{(QL)}, \quad \mathcal{M}_{\bar{K}^0 K^0}^{(MP)} = \mathcal{M}_{K^+K^-}^{(MP)}, \quad (29)$$

where the terms proportional to  $r_\pi r_K$  or  $r_K^2$  are not shown for the sake of simplicity. The functions  $h_e, h_g$  and  $h'_g$ , the hard scales  $t_a$  and  $t_b$ , as well as the Sudakov factors  $S_{ab}(t)$  and  $S_{cd}(t)$  in Eqs.(24-28) will be given in Appendix A.

#### IV. NUMERICAL RESULTS

In the numerical calculations the following input parameters will be used.

$$\begin{aligned} \Lambda_{\overline{\text{MS}}}^{(5)} &= 0.225\text{GeV}, & f_{B_s} &= (0.23 \pm 0.02)\text{GeV}, & f_K &= 0.16\text{GeV}, & f_\pi &= 0.13\text{GeV}, \\ M_{B_s} &= 5.37\text{GeV}, & m_K &= 0.494\text{GeV}, & m_0^\pi &= 1.4\text{GeV}, & m_0^K &= 1.9\text{GeV}, \\ \tau_{B_s^0} &= 1.497\text{ps}, & m_b &= 4.8\text{GeV}, & M_W &= 80.42\text{GeV}. \end{aligned} \quad (30)$$

For the CKM matrix elements, we also take the same values as being used in Ref. [5], and neglect the small errors on  $V_{ud}, V_{us}, V_{ts}$  and  $V_{tb}$

$$\begin{aligned} |V_{ud}| &= 0.974, & |V_{us}| &= 0.226, & |V_{ub}| &= (3.68_{-0.08}^{+0.11}) \times 10^{-3}, \\ |V_{td}| &= (8.20_{-0.27}^{+0.59}) \times 10^{-3}, & |V_{ts}| &= 40.96 \times 10^{-3}, & |V_{tb}| &= 1.0, \\ \alpha &= (99_{-9.4}^{+4})^\circ, & \gamma &= (59.0_{-3.7}^{+9.7})^\circ, & \arg[-V_{ts}V_{tb}^*] &= 1^\circ. \end{aligned} \quad (31)$$

##### A. Branching Ratios

For the considered  $B_s^0$  decays, the decay amplitude for a given decay mode with  $b \rightarrow d, s$  transitions can be generally written as

$$\mathcal{A}(\bar{B}_s^0 \rightarrow f)|_{b \rightarrow d} = V_{ub}V_{ud}^*T - V_{tb}V_{td}^*P = V_{ub}V_{ud}^*T [1 + ze^{i(-\alpha+\delta)}], \quad (32)$$

$$\mathcal{A}(\bar{B}_s^0 \rightarrow f)|_{b \rightarrow s} = V_{ub}V_{us}^*T' - V_{tb}V_{ts}^*P' = V_{ub}V_{us}^*T' [1 + z'e^{i(\gamma+\delta')}], \quad (33)$$

where  $\alpha$  and  $\gamma$  are the weak phase ( the CKM angles ),  $\delta = \arg[P/T]$  and  $\delta' = \arg[P'/T']$  are the relative strong phase between the tree (T) and penguin (P) diagrams, and the parameter “z” is the ratio of penguin to tree contributions with the definition

$$z = \left| \frac{V_{tb}V_{td}^*}{V_{ub}V_{ud}^*} \right| \left| \frac{P}{T} \right|, \quad z' = \left| \frac{V_{tb}V_{ts}^*}{V_{ub}V_{us}^*} \right| \left| \frac{P'}{T'} \right|. \quad (34)$$

The ratio  $z$  and the strong phase  $\delta$  can be calculated in the pQCD approach. The CP-averaged branching ratio, consequently, can be defined as

$$\text{Br}(\bar{B}_s^0 \rightarrow f) = \frac{G_F^2 \tau_{B_s^0}}{32\pi m_B} \frac{1}{2} [|\mathcal{A}(\bar{B}_s^0 \rightarrow f)|^2 + |\mathcal{A}(B_s^0 \rightarrow \bar{f})|^2], \quad (35)$$

where  $\tau_{B_s^0}$  is the lifetime of the  $B_s^0$  meson.

In Table I, we list the pQCD predictions for the branching ratios of the four  $B_s^0 \rightarrow K\pi, KK$  decays. The label “LO” and “NLO” means the pQCD predictions at the leading order and with the inclusion of all currently known NLO contributions. The label “Set-A” means the pQCD predictions without the inclusion of the newly known NLO twist-2 and twist-3 contributions to the form factors of  $B \rightarrow K$  transitions. For the sake of comparison, we also show the LO pQCD predictions as given in Ref. [5] in the fourth column, and list the NLO theoretical predictions obtained

TABLE I. The pQCD predictions for the branching ratios ( in units of  $10^{-6}$ ) of the four  $B_s^0 \rightarrow K\pi, KK$  decays. The label ‘‘LO’’ and ‘‘NLO’’ means the leading order and the full next-to-leading order pQCD predictions, while ‘‘Set-A’’ means only NLO twist-2 and twist-3 contributions to form factors are not taken into account. The values listed in the fifth, sixth and seventh column are the LO pQCD predictions [5], the QCDF predictions [8], and currently available data [25, 26].

Mode	Class	LO	pQCD [5]	Set-A	NLO	QCDF [8]	Data
$\bar{B}_s^0 \rightarrow K^+\pi^-$	T	7.30	$7.6^{+3.3}_{-2.5}$	6.4	$5.7^{+2.2+0.5+0.2}_{-1.7-0.6-0.3}$	$10.2^{+6.0}_{-5.2}$	$5.4 \pm 0.6$
$\bar{B}_s^0 \rightarrow K^0\pi^0$	C	0.19	$0.16^{+0.12}_{-0.07}$	0.30	$0.28^{+0.10+0.03+0.02}_{-0.06-0.02-0.01}$	$0.49^{+0.62}_{-0.35}$	
$\bar{B}_s^0 \rightarrow K^+K^-$	P	13.1	$13.6^{+8.6}_{-5.2}$	20.3	$19.7^{+6.2+2.4+0.2}_{-4.8-2.2-0.2}$	$22.7^{+27.8}_{-13.0}$	$24.5 \pm 1.8$
$\bar{B}_s^0 \rightarrow \bar{K}^0K^0$	P	13.3	$15.6^{+9.7}_{-6.0}$	21.2	$20.2^{+6.5+2.4+0.0}_{-4.9-2.2-0.0}$	$24.7^{+29.4}_{-14.0}$	

by employing the QCD factorization approach as given in Ref. [8] in the seventh column. The corresponding errors of the previous LO pQCD predictions [5] and the QCDF predictions[8] are the combined total errors. The currently available experimental measurements [25, 26] are also shown in the last column of Table I.

The theoretical errors of the NLO pQCD predictions as shown in the sixth column of Table I are induced by the uncertainties of the input parameters. The first dominant error comes from  $\omega_b = 0.50 \pm 0.05$  and  $f_{B_s} = 0.23 \pm 0.02$  GeV, added in quadrature. The second error arises from the uncertainties of the CKM matrix elements  $|V_{ub}|$  and  $|V_{cb}|$ , as well as the CKM angles  $\alpha$  and  $\gamma$  as given in Eq. (31). The third error comes from the uncertainties of relevant Gegenbauer moments:  $a_1^K = 0.17 \pm 0.05$ ,  $a_2^K = 0.20 \pm 0.06$  and  $a_2^\pi = 0.44^{+0.10}_{-0.20}$ , added in quadrature again. We here assigned roughly a 30% uncertainty for Gegenbauer moments to estimate the resultant errors for the pQCD predictions of the branching ratios.

From the numerical results of the branching ratios, we have the following observations:

1. The LO pQCD predictions for the branching ratios as given in Ref. [5] are confirmed by our independent calculations. The small differences between the values in column three and four are mainly induced by the different choices of the scales  $\Lambda_{QCD}^{(4)}$  and  $\Lambda_{QCD}^{(5)}$ : we take  $\Lambda_{QCD}^{(5)} = 0.225$  GeV and  $\Lambda_{QCD}^{(4)} = 0.287$  GeV, instead of the values of  $\Lambda_{QCD}^{(5)} = 0.193$  GeV and  $\Lambda_{QCD}^{(4)} = 0.25$  GeV as being used in Ref. [5].
2. The NLO contributions can interfere with the LO part constructively or destructively for different decay modes. The inclusion of NLO contributions can leads to a better agreement between the theoretical predictions and currently available measured values.
3. The  $\bar{B}_s^0 \rightarrow K^+\pi^-$  decay is a ‘‘tree’’ dominated decay mode, the NLO contribution leads to a 22% decrease to the LO pQCD prediction only. For other three ‘‘Color-suppressed’’ and ‘‘QCD-penguin’’ decay modes, however, the NLO contribution leads to a  $\sim 50\%$  enhancement to the LO ones, which in turn play an important role in interpreting the observed large branching ratio  $Br(B_s^0 \rightarrow K^+K^-) = (24.5 \pm 1.8) \times 10^{-6}$  [25, 26].

## B. CP-violating asymmetries

Now we turn to the evaluations of the CP-violating asymmetries of the considered four  $B_s^0$  decays in the pQCD approach. For  $B_s^0 \rightarrow K^\mp\pi^\pm$  decays, the definition for its direct CP violating

TABLE II. The same format as in Table I, but for the pQCD predictions (in unit of  $10^{-2}$ ) for the direct CP asymmetries  $\mathcal{A}_f$ . The previous LO pQCD predictions [5], the QCDF predictions [8] and the measured values [1, 2] are also listed.

Mode	Class	LO	pQCD [5]	Set-A	NLO	QCDF [8]	Data
$\bar{B}_s^0 \rightarrow K^+\pi^-$	$T$	27.6	$24.1^{+5.6}_{-4.8}$	36.2	$38.7^{+5.0+2.1+2.2}_{-5.0-1.8-1.8}$	$-6.7^{+15.6}_{-15.3}$	$27 \pm 4[1]$
$\bar{B}_s^0 \rightarrow K_S^0\pi^0$	$C$	62.9	$59.4^{+7.9}_{-12.5}$	84.8	$83.0^{+5.8+3.4+2.3}_{-5.6-2.6-2.7}$	$42^{+47}_{-56}$	
$\bar{B}_s^0 \rightarrow K^+K^-$	$P$	-13.7	$-23.3^{+5.0}_{-4.6}$	-17.1	$-16.4^{+0.3+0.6+0.6}_{-0.1-0.4-0.6}$	$4.0^{+10.6}_{-11.6}$	$-14 \pm 12[2]$
$\bar{B}_s^0 \rightarrow \bar{K}^0K^0$	$P$	0	0	-0.7	$-0.7 \pm 0.1$	$0.3 \pm 0.1$	

asymmetry is very simple[1]. For neutral  $B_s^0$  decays into a CP eigenstate  $\bar{f} = \eta_{CP}f$  with  $\eta_{CP} = \pm 1$  for the CP-even and CP-odd final states, the time dependent CP asymmetry can be defined as [2, 27]

$$\mathcal{A}(t) = \frac{\Gamma_{\bar{B}_s^0 \rightarrow f}(t) - \Gamma_{B_s^0 \rightarrow f}(t)}{\Gamma_{\bar{B}_s^0 \rightarrow f}(t) + \Gamma_{B_s^0 \rightarrow f}(t)} = \frac{\mathcal{A}_f \cos(\Delta m_s t) + \mathcal{S}_f \sin(\Delta m_s t)}{\cosh\left(\frac{\Delta\Gamma_s t}{2}\right) + \mathcal{H}_f \sinh\left(\frac{\Delta\Gamma_s t}{2}\right)}, \quad (36)$$

where  $\Delta m_s$  and  $\Delta\Gamma_s$  are the mass and width differences of the  $B_s^0 - \bar{B}_s^0$  system mass eigenstates. The direct CP violating asymmetry  $\mathcal{A}_f$ , the mixing-induced CP violating asymmetry  $\mathcal{S}_f$  and  $\mathcal{H}_f$  are defined as in Refs. [2, 27]:

$$\mathcal{A}_f = \frac{|\lambda_f|^2 - 1}{1 + |\lambda_f|^2}, \quad \mathcal{S}_f = \frac{2\text{Im}\lambda_f}{1 + |\lambda_f|^2}, \quad \mathcal{H}_f = \frac{2\text{Re}\lambda_f}{1 + |\lambda_f|^2}, \quad (37)$$

where the three factors satisfy the normalization relation:  $|\mathcal{A}_f|^2 + |\mathcal{S}_f|^2 + |\mathcal{H}_f|^2 = 1$ , and the CP-violating parameter  $\lambda_f$  is defined as

$$\lambda_f = \frac{q}{p} \frac{\bar{A}_f}{A_f} = \eta_f e^{2i\epsilon} \frac{A(\bar{B}_s \rightarrow f)}{A(B_s \rightarrow f)} \quad (38)$$

where  $\epsilon = \arg[-V_{ts}V_{tb}^*]$  is very small in size and can be neglected safely. It is worth of mentioning that the parameter  $\mathcal{A}_f$  and  $\mathcal{H}_f$  defined in Eqs. (36,37) have opposite sign with the parameter  $\mathcal{C}_f$  and  $\mathcal{A}_f^{\Delta\Gamma}$  as defined in Ref.[2]: i.e.,  $\mathcal{A}_f = -\mathcal{C}_f$  and  $\mathcal{H}_f = -\mathcal{A}_f^{\Delta\Gamma}$ .

In Table II and III, we list the pQCD predictions (in unit of  $10^{-2}$ ) for the direct CP-violating asymmetry  $\mathcal{A}_f$ , the mixing-induced CP-violating asymmetry  $\mathcal{S}_f$  and  $\mathcal{H}_f$  of the considered  $B_s^0$  decays, respectively. As a comparison, the LO pQCD predictions as given in Ref. [5], the QCDF predictions as given in Ref. [8, 9] and the measured values [1, 2] are listed in Table II and Table III. The errors of our NLO pQCD predictions for CP-violating asymmetries are defined in the same way as those for the branching ratios.

From the pQCD predictions and currently available data for the CP violating asymmetries of the considered  $\bar{B}_s^0$  decays, we find that (a) the LO pQCD predictions obtained in this paper agree well with those as given in Ref. [5]; (b) For the CP-violating asymmetries of the considered  $\bar{B}_s^0$  decays, the effects of the NLO contributions are small or moderate in size; and (c) for  $\bar{B}_s^0 \rightarrow K^\pm\pi^\mp$  and  $\bar{B}_s^0 \rightarrow K^+K^-$  decays, the pQCD predictions for both  $\mathcal{A}_f$  and  $\mathcal{S}_f$  agree well with those measured values in both the sign and the magnitude.

TABLE III. The same format as in Table I, but for the pQCD predictions (in unit of  $10^{-2}$ ) for the mixing-induced CP asymmetries  $\mathcal{S}_f$  and  $\mathcal{H}_f$  (the second row). The previous LO pQCD predictions [5], the QCDF predictions [9] and the measured values [1, 2] are also listed.

Mode	Class	LO	pQCD [5]	Set-A	NLO	QCDF[9]	Data[2]
$\bar{B}_s^0 \rightarrow K_S^0 \pi^0$	C	-56.2	$-61^{+24}_{-20}$	-50.0	$-52.9^{+8.0+4.2+4.7}_{-8.2-4.3-4.4}$	45	
		-53.7	$-52^{+23}_{-17}$	-17.8	$-17.4^{+0.9+2.0+4.8}_{-0.1-1.0-4.1}$	-	
$\bar{B}_s^0 \rightarrow K^+ K^-$	P	37.1	$28^{+5}_{-5}$	22.0	$20.6^{+1.9+1.4+0.8}_{-1.8-1.3-0.7}$	27	$30 \pm 13$
		92.0	$93^{+3}_{-3}$	96.0	$96.5^{+0.3+0.1+0.1}_{-0.4-0.2-0.2}$	-	
$\bar{B}_s^0 \rightarrow \bar{K}^0 K^0$	P	-	4	-0.2	-0.2	-3.5	
		100	$\sim 100$	$\sim 100$	$\sim 100$	-	

## V. SUMMARY

In this paper, we calculated the branching ratios and CP-violating asymmetries of the four  $\bar{B}_s^0 \rightarrow K\pi, KK$  decays, with the inclusion of all known NLO contributions, especially the NLO twist-2 and twist-3 contributions to the form factors to  $B_s \rightarrow K$  transition. From our calculations and phenomenological analysis, we found the following results:

1. For the considered four decays, the NLO contribution can interfere with the LO part constructively or destructively for different decay modes. The currently available data can be interpreted by the inclusion of the NLO contribution.
2. For  $Br(\bar{B}_s^0 \rightarrow K^+ \pi^-)$ , the NLO contribution leads to a 22% decrease to the LO pQCD prediction. For other three decay modes, however, the NLO contributions can provide  $\sim 50\%$  enhancements to the LO ones and therefore play an important role in interpreting the observed large branching ratio  $Br(\bar{B}_s^0 \rightarrow K^+ K^-) = (24.5 \pm 1.8) \times 10^{-6}$ .
3. For the CP-violating asymmetries, the effects of the NLO contributions are small or moderate in size. For  $\bar{B}_s^0 \rightarrow K^+ \pi^-$  and  $\bar{B}_s^0 \rightarrow K^+ K^-$  decays, the pQCD predictions for the direct and mixing induced CP-violating asymmetries agree very well with the measured values in both the sign and the magnitude.

## ACKNOWLEDGMENTS

This work is partly supported by the National Natural Science Foundation of China under Grant No.11235005.

## Appendix A: Related hard functions and Sudakov factors

We here list the hard function  $h_i$  and the Sudakov factors  $S_{ab}(t)$  and  $S_{cd}(t)$  appeared in the expressions of the decay amplitudes in Eqs. (24-28). The hard functions  $h_i(x_j, b_j)$  are obtained by making the Fourier transformations of the hard kernel  $H^{(0)}$ .

$$\begin{aligned}
 h_e(x_1, x_3, b_1, b_3) = & \left[ \theta(b_1 - b_3) I_0(\sqrt{x_3} m_{B_s} b_3) K_0(\sqrt{x_3} m_{B_s} b_1) + \theta(b_3 - b_1) I_0(\sqrt{x_3} m_{B_s} b_1) \right. \\
 & \left. \cdot K_0(\sqrt{x_3} m_{B_s} b_3) \right] \cdot K_0(\sqrt{x_1 x_3} m_{B_s} b_1) S_t(x_3), \tag{A1}
 \end{aligned}$$

$$h_g(x_i, b_i) = -\frac{i\pi}{2} S_t(x_3) \left[ J_0(\sqrt{x_2 \bar{x}_3} m_{B_s} b_2) + i N_0(\sqrt{x_2 \bar{x}_3} m_{B_s} b_2) \right] \cdot K_0(\sqrt{x_1 x_3} m_{B_s} b_1) \cdot \int_0^{\pi/2} d\theta \tan \theta \cdot J_0(\sqrt{x_3} m_{B_s} b_1 \tan \theta) J_0(\sqrt{x_3} m_{B_s} b_2 \tan \theta) \cdot J_0(\sqrt{x_3} m_{B_s} b_3 \tan \theta), \quad (\text{A2})$$

$$h'_g(x_i, b_i) = -S_t(x_1) K_0(\sqrt{x_1 x_3} m_{B_s} b_3) \cdot \int_0^{\pi/2} d\theta \tan \theta \cdot J_0(\sqrt{x_1} m_{B_s} b_1 \tan \theta) \cdot J_0(\sqrt{x_1} m_{B_s} b_2 \tan \theta) J_0(\sqrt{x_1} m_{B_s} b_3 \tan \theta) \times \begin{cases} \frac{i\pi}{2} [J_0(\sqrt{x_2 - x_1} m_{B_s} b_2) + i N_0(\sqrt{x_2 - x_1} m_{B_s} b_2)], & x_1 < x_2, \\ K_0(\sqrt{x_1 - x_2} m_{B_s} b_2), & x_1 > x_2, \end{cases} \quad (\text{A3})$$

with  $K_0$ ,  $I_0$  and  $J_0$  are the Bessel functions [28]. And the threshold resummation form factor  $S_t(x_i)$  can be found in Ref. [24].

The Sudakov factors appeared in Eqs. (24-28) are defined as

$$S_{ab}(t) = s\left(x_1 \frac{m_{B_s}}{\sqrt{2}}, b_1\right) + s\left(x_3 \frac{m_{B_s}}{\sqrt{2}}, b_3\right) + s\left(\bar{x}_3 \frac{m_{B_s}}{\sqrt{2}}, b_3\right) + \frac{5}{3} \int_{1/b_1}^t d\mu \frac{\gamma_q(\alpha_s(\mu))}{\mu} + 2 \int_{1/b_3}^t d\mu \frac{\gamma_q(\alpha_s(\mu))}{\mu}, \quad (\text{A4})$$

$$S_{cd}(t) = s\left(x_1 \frac{m_{B_s}}{\sqrt{2}}, b_1\right) + s\left(x_2 \frac{m_{B_s}}{\sqrt{2}}, b_2\right) + s\left(\bar{x}_2 \frac{m_{B_s}}{\sqrt{2}}, b_2\right) + s\left(x_3 \frac{m_{B_s}}{\sqrt{2}}, b_1\right) + s\left(\bar{x}_3 \frac{m_{B_s}}{\sqrt{2}}, b_1\right) + \frac{11}{3} \int_{1/b_1}^t d\mu \frac{\gamma_q(\alpha_s(\mu))}{\mu} + 2 \int_{1/b_2}^t d\mu \frac{\gamma_q(\alpha_s(\mu))}{\mu}, \quad (\text{A5})$$

where  $\bar{x}_i = 1 - x_i$ , the function  $s(Q, b)$  can be found in Refs. [29, 30]. The hard scales  $t_a$  and  $t_b$  appeared in Eqs. (24-28) take the form of

$$t_a = \max \left\{ \sqrt{x_1 x_3} m_{B_s}, \sqrt{x_3} m_{B_s}, \sqrt{x_2(1-x_3)} m_{B_s}, 1/b_1, 1/b_3 \right\}, \\ t_b = \max \left\{ \sqrt{x_1 x_3} m_{B_s}, \sqrt{x_1} m_{B_s}, \sqrt{|x_1 - x_2|} m_{B_s}, 1/b_1, 1/b_3 \right\}, \quad (\text{A6})$$

where the energy scale  $\sqrt{x_2(1-x_3)} m_{B_s}$  and  $\sqrt{|x_1 - x_2|} m_{B_s}$  come from the invariant mass of the gluon  $l^2 = x_2(1-x_3) m_{B_s}^2$  and  $l'^2 = (x_1 - x_2) m_{B_s}^2$ . They are chosen as the maximum energy scale appearing in each diagram to kill the large logarithmic radiative corrections.

- 
- [1] R. Aaij *et al.* (LHCb Collaboration), Phys. Rev. Lett. **108**, 201601 (2012); R. Aaij *et al.* (LHCb collaboration), Phys. Rev. Lett. **110**, 221601 (2013).  
[2] R. Aaij *et al.* (LHCb collaboration), J. High Energy Phys. **10**, 183 (2013); Phys. Lett. B **716**, 393(2012).  
[3] Y. Li, C.D. Lü, Z.J. Xiao, and X.Q. Yu, Phys. Rev. D **70**, 034009 (2004); X.Q. Yu, Y. Li, and C.D. Lü, Phys. Rev. D **71**, 074026 (2005); Phys. Rev. D **73**, 017501 (2006); J. Zhu, Y.L. Shen, and C.D. Lü, J. Phys. G **32**, 101 (2006).

- [4] Z.J. Xiao, X. Liu and H.S. Wang, Phys. Rev. D **75**, 034017 (2007).
- [5] A. Ali, G. Kramer, Y. Li, C.D. Lü, Y.L. Shen, W. Wang and Y.M. Wang, Phys. Rev. D **76**, 074018 (2007).
- [6] J.Liu, R.Zhou and Z.J. Xiao, [arXiv:0812.2312](#)[hep-ph].
- [7] Y.H. Chen, H.Y. Cheng, B. Tseng, Phys. Rev. D **59**, 074003 (1999).
- [8] M. Beneke and M. Neubert, Nucl. Phys. B **675**, 333 (2003).
- [9] J.F. Sun, G.H. Zhu, D.S. Du, Phys. Rev. D **68**, 054003 (2003).
- [10] H.Y. Cheng and C.K. Chua, Phys. Rev. D **80**, 114026 (2009).
- [11] Z.J. Xiao, Z.Q. Zhang, X. Liu, and L.B. Guo, Phys. Rev. D **78**, 114001 (2008).
- [12] Y.Y. Fan, W.F. Wang, S.Cheng, and Z.J. Xiao, Phys. Rev. D **87**, 094003 (2013).
- [13] W. Bai, M. Liu, Y.Y. Fan, W.F. Wang, S. Cheng, and Z.J. Xiao, Chin. Phys. C **38**, 033101(2014).
- [14] H.N. Li, S. Mishima, A.I. Sanda, Phys. Rev. D **72**, 114005 (2005).
- [15] H.N. Li, Y.L. Shen, and Y.M. Wang, Phys. Rev. D **85**, 074004 (2012).
- [16] S. Cheng, Y.Y. Fan, X. Yu, C.D. Lü and Z.J. Xiao, [arXiv:1402.5501v2](#)[hep-ph].
- [17] H.N. Li, Prog. Part. & Nucl. Phys. **51**, 85 (2003) and references therein.
- [18] G. Buchalla, A.J. Buras, M.E. Lautenbacher, Rev. Mod. Phys.**68**, 1125 (1996).
- [19] V.M. Braun and I.E. Filyanov , Z. Phys. C **48**, 239 (1990); P. Ball, V.M. Braun, Y. Koike, and K. Tanaka, Nucl. Phys. B **529**, 323 (1998); P. Ball, J. High Energy Phys. **01**, 010 (1999).
- [20] V.M. Braun and A. Lenz, Phys. Rev. D **70**, 074020 (2004); P. Ball and A. Talbot, J. High Energy Phys. **06**, 063 (2005); P. Ball and R. Zwicky, Phys. Lett. B **633**, 289 (2006); A. Khodjamirian, Th. Mannel, and M. Melcher, Phys. Rev. D **70**, 094002 (2004).
- [21] X.G. Wu and T. Huang, [arXiv:1312.1355](#)[hep-ph].
- [22] S. Mishima and A.I. Sanda, Prog. Theor. Phys. **110**, 549 (2003).
- [23] M. Beneke, G. Buchalla, M. Neubert and C.T. Sachrajda, Phys. Rev. Lett. **83**, 1914 (1999); Nucl. Phys. B **591**, 313 (2000).
- [24] T. Kurimoto, H.N. Li, and A.I. Sanda, Phys. Rev. D **65**, 014007 (2001); C.D. Lu and M.Z. Yang, Eur. Phys. J. C **28**, 515 (2003).
- [25] Y. Amhis *et al.*, (Heavy Flavor Averaging Group), [arXiv:1207.1158](#) [hep-ex].
- [26] J. Beringer *et al.* (Particle Data Group), Phys. Rev. D **86**, 010001 (2012).
- [27] I. Dunietz, Phys. Rev. D **52**, 3048 (1995).
- [28] I.S. Gradshteyn and I.M. Ryzhik, Table of Integrals, Series, and Products, Academic Press, 1980.
- [29] H.N. Li and K.Ukai, Phys. Lett. B **555**, 197(2003).
- [30] H.N. Li and B. Melic, Eur. Phys. J. C **11**, 695 (1999).